Independent validation of a system for real-time localization of the prostate during motion tracking radiotherapy

Klara Stefansson
Main supervisor: André Änghede Haraldsson
Supervisor: Per Munck af Rosenschöld

Autumn 2023

LUNDS
UNIVERSITET

Abstract

Intrafractional prostate motion during external beam radiotherapy of prostate tumors has been reported as a limiting factor in accurate treatment delivery. Technology for real-time image-guided radiotherapy has been introduced for tracking and for compensating prostate motion during treatment and could allow for reduced target margins. This project investigated the geometrical accuracy of Radixact Synchrony, an image-guided Multi Leaf Collimator-tracking system, in its detection of intrafractional translational prostate motion by comparison with Kilovoltage Intrafractional Monitoring (KIM), an independent retrospective model for trajectory estimation using 2D-kVs. KIM's and Synchrony's estimations of prostate trajectories in a phantom reproducing previously recorded tumor trajectories were compared to the known phantom trajectories. For clinical validation in patients, KIM retrospectively estimated the clinical tumor trajectories at a total of 41 fractions for seven prostate cancer patients using the 2D-kV images acquired by Synchrony during treatment. The KIM-estimated trajectories were then compared to the trajectories estimated by Synchrony. Synchrony's ability to detect uncertainty in its estimations, as reflected in the built-in uncertainty parameter Potential difference, was analyzed. The results showed that KIM's estimations of phantom trajectories were accurate, establishing its validity for verifying Synchrony's estimations in patients. Estimation differences between KIM and Synchrony mainly appeared in conjunction with rapid movement in the form of oscillations in Synchrony's estimation of the left-right prostate motion and a delay in Synchrony's estimation of the anterior-posterior prostate motion. Errors were transient and reflected in an increase of Potential difference, implying a low impact on delivered dose and a capability of the system to detect estimation uncertainties. The results lead to the conclusion that Synchrony accurately estimates the intrafractional translational motion and could be used to reduce target margins during treatment.

Contents

1 List of Abbreviations

2D-kV: Image taken using a keV source
AP: Motion axis: Anterior-Posterior
CC: Motion axis: Cranio-Caudal
CT: Computed Tomography
CTV: Clinical Target Volume
KIM: Kilovoltage Intrafractional Monitoring
LR: Motion axis: Left-Right
MR: Magnetic Resonance
MLC: Multi Leaf Collimator
PDF: Probability Density Function
PTV: Planned Target Volume
RMSD: Root-mean-square difference
SD: Standard deviation

2 Introduction

Radiation has been used to treat cancer ever since the discovery of radioactivity, and one of the cancer forms that was earliest subject to trying this new form of treatment was prostate cancer. Ten years after the discovery of radium by Pierre and Marie Curie, Henri Minet published his results from inserting radium-containing tubes into the urethra in an attempt to treat prostate cancer [1]. The principle behind the treatment of cancer using radiotherapy is to kill or slow the growth of cancer cells by damaging their DNA. The radiation can be delivered internally through Brachytherapy or liquid sources orally, intravenously or injected, or externally by external beam radiotherapy [2]. Radiation is non selective and doesn't differentiate between healthy and cancer cells, thus having the potential to cause harm to healthy tissues as well as to the tumor. Therefore, finding ways to direct the treatment to the tumor and sparing as much of the healthy sorrounding tissues as possible is one of the important challenges in cancer treatment using radiotherapy.

2.1 Radiotherapy treatment of prostatic tumors

The prostate is a gland in the male body that produces components of the seminal plasma. It is located in the pelvis below the urine bladder, between the pubic bone and the rectum. The urethra passes trough the prostate on its way from bladder to meatus, see figure 1. The surrounding organs all provide vital functions and are, together with the femoral heads, considered so called organs at risk during treatment of prostate tumors. This means that efforts to spare these organs from irradiation will be made during treatment planning [3].

When a patient is diagnosed with prostate cancer, the whole prostate is considered malignant tissue and radiation is delivered to the entire organ. A physician identifies and delineates the clinical tumor volume (CTV) which consists of the tumor and additional suspected malignant tissue in patient images and prescribes a certain radiation dose [3]. In order to facilitate prostate position identification throughout the treatment period, three golden markers, called fiducials, are often implanted in the prostate after diagnosis [4].

The target volume is expanded into the planning target volume (PTV) to create a margin for uncertainties in treatment delivery. Today, the margin used during treatment of prostate tumors at the University Hospital in Skåne is 7 mm. A medical phycisist then plans the treatment session using an optimization software that finds the optimal delivery configuration for the desired dose distribution [5]. A dose distribution for treatment of a prostate tumor can be seen in figure 2. Radiation used during external radiotherapy

of the prostate are high-energy X-rays in the MeV spectrum created by accelerating electrons in a linear accelerator (Linac) and directing them at a metal target. When interacting with the material of the target, the electrons are slowed down and X-rays are emitted [6].

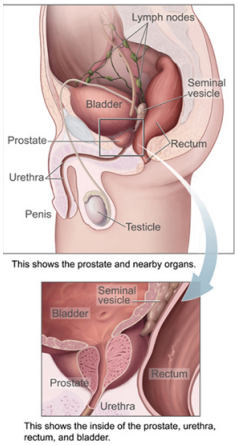

Figure 1: The anatomical location of the prostate. Image source: US government agency National Cancer Institute [7]

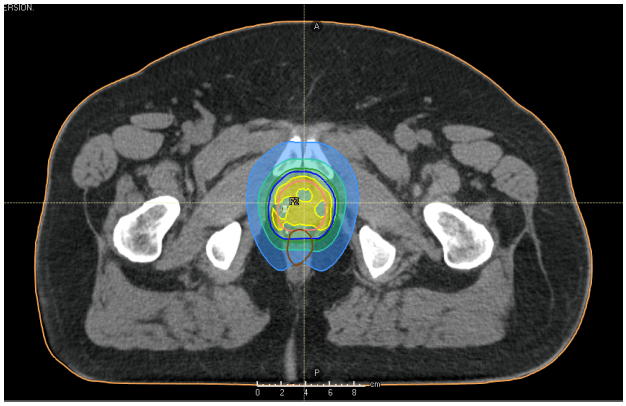

Figure 2: An example of a dose plan created for prostate cancer treatment. Image source: André Änghede Haraldsson, with permission.

The treatment delivery and thus the distribution of delivered dose can be modulated in many ways: the shape of the radiation beam can be changed into arbitrary shapes by using collimators and the intensity of the radiation beam can be modulated throughout the treatment sessions. In addition, the radiation source is mounted on a gantry that can move around the patient and thus deliver radiation from several different angles, see figure 3. The treatment is often fractionated into several sessions, called fractions [3].

The patient is treated laying down in back position on a table mounted on the treatment unit. Prior to each treatment fraction, the patient position is adapted to ensure treatment delivery to the tumor. This is done by modifying the table position after computed tomography imaging done in conjunction with each tratment fraction [4].

Due to the importance of correct positioning and that several components of the treatment unit are mobile, there are several coordinate systems defined to ensure clear communication of postition adaptions needed. The aspects of radiotherapy treatment discussed in this report all occur in the patient coordinate system, which is defined in figure 4. Motion along the x-axis will be referred to as left-right (LR) motion, motion along the y-axis will be referred to as cranio-caudal (CC) motion and motion along the z-axis will be referred to as anterio-posterior (AP) motion.

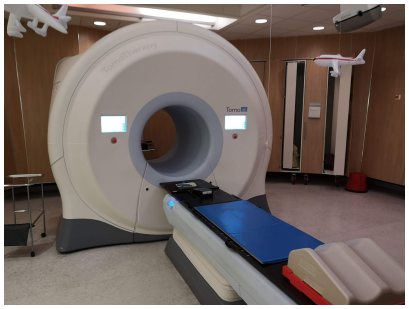

Figure 3: A radiotherapy treatment delivery system. Image source: André Änghede Haraldsson, with permission.

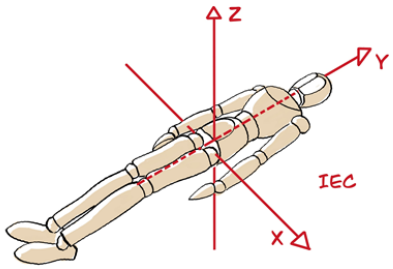

Figure 4: The patient coordinate system. Illustration by Per E. Engström, with permission

2.1.1 Geometrical uncertainties in treatment of prostate tumors

There are several sources of geometrical uncertainties during treatment of prostate tumors. The tumor delineation can introduce errors caused by both human factors in i.e. the assesment of what should be included in the CTV as well as errors introduced by the imaging system. Due to the ability of magnetic resonance (MR) imaging to depict contrast in soft tissue, MR-produced images are preferred for delineation. However, computed tomography (CT) images are used for dose calculation during treatment planning as the image intensity of CTs reflects the radiation absorbtion of the tissue. The MR images are therefore converted into so called synthetic CTs after CTV delineation using a specific software. In this conversion, there is some uncertainty in the identification of the fiducial marker positions which has been seen to introduce a systematic displacement of the identified tumor position of up to 2 mm throughout all treatment fractions [8].

Errors in the positioning of the patient for each fraction could also introduce further uncertainty in delivered dose. In addition, the prostate is not a static organ and can move both between fractions (interfractional tumor motion) and within fractions (intrafractional tumor motion). The interfractional motion can be accounted for to some extent during patient setup [3]. This project will study a system which monitors and adjusts treatment in response to intrafractional tumor motion.

2.1.2 Intrafractional prostate tumor motion

The rectum and the bladder can both change size within very short time periods as they are filled or gas passes through the gastro-intestinal canal. Since the prostate is localized in close proximity to these organs, the movements and size changes of the rectum and bladder translates to movements of the prostate. The main part of prostate motion is

attributed to rectal filling. Typically, the movements are smaller than 5 mm, but the prostate has been measured to move as much as 18 mm [9]. Motion usually occurs in the CC- and AP directions, with a correlation between the two directions of motion. Motion in LR is typically small and not well correlated with motion in the other motion directions [10]. The prostate has also known to rotate, however this project will only look at the system's detection of translational movements.

2.2 Real-time target tracking and motion management

To account for and adapt the radiation beam to the motion of the prostate and thus allow for reduced target margins in the PTV, several techniques for real-time motion management have been introduced. The motion management consists of two parts: identifying the current tumor position, and adapting the radiation beam geometry and direction to this found tumor position. One common method for enabling tracking of the tumor position throughout the treatment fractions is mounting a generator of radiation in the keV spectrum perpendicular to the MeV producing Linac, with an imager plate on the opposite side of the gantry. This allows for 2D-kV images being taken throughout treatment [3].

2D-kV images obtained during treatment by the rotating imager provide information about the intrafractional positions of the fiducials. One such 2D-kV image is seen in figure 5. If the tumor were static, the information from two such images would be enough to triangulate and thus exactly determine the tumor position. However, the position of a moving tumor could not be unambigously determined since the motion that has occurred in the direction parallell to the imager axis between imaging time points can not be determined from the projected positions. An inifinite number of trajectories could generate the set of projections obtained, which is the greatest cause of uncertainty when transforming the projected 2D positions into the 3D position of the tumor [10].

When the tumor position has been determined, the treatment beam is collimated and shaped to the desired radiation field shape using collimator jaws and a multileaf collimator (MLC). The collimator jaws are two tungsten blocks creating a rectangular field shape and the MLC consists of several tungsten alloy leaves which can move independantly of each other and create more arbitrary shapes of the treatment beam, see figure 6 [3].

Movement parallell to the treatment beam has negligable effects on the dose delivered to the tumor whereas movements in directions perpendicular to the beam potentially could move the tumor outside of the PTV. Since the imager axis in most image guided radiotherapy systems is mounted perpendicular to the treatment beam, the uncertainty

in the position parallell to the imager axis is directly realted to an uncertainty in the delivered dose. This poses a great challenge for image guided radiotherapy systems and the system's strategy for determining the unknown motion component as well as its knowledge about its limitations and uncertainty in this estimation is essential for patient safety [10].

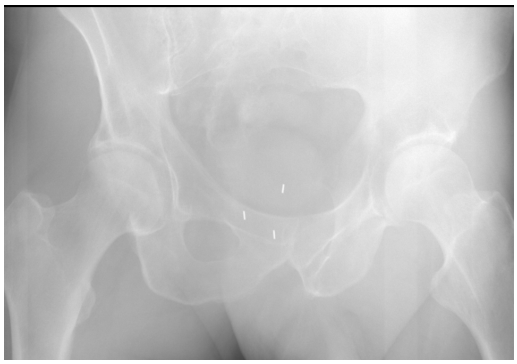

Figure 5: A 2D-kV image of a prostate with three implanted golden fiducials

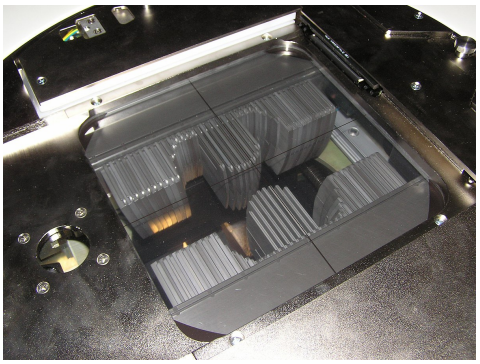

Figure 6: A multi leaf collimator (MLC). Image source: Wikimedia Commons [11]

2.3 Radixact Synchrony

Radixact Synchrony uses sequential monoscopic imaging and statistical modelling to estimate the intrafractional motion of tumors with implanted fiducials. It combines the 2D information of the tumor position in the sequential 2D-kVs obtained during treatment to determine the current tumor position and collimates the treatment beam accordingly using Jaws and MLC.

2.3.1 Synchrony's estimation of target position

The fiducial position is segmented from the 2D-kVs by matching the expected appearance of the fiducials based on the digitally reconstructed 2D-kV from the pre-treatment CT whithin a defined search area. The center of the search area is established by the expected position of the fiducials at the beginning of treatment and thereafter by the Synchrony estimated positions. The system identifies fiducial candidates within each search area and selects the candidates that best preserve the spatial relationship between the fiducials compared to the plan as the fiducial position [12].

The 3D tumor position is then estimated using statistical modeling based on the 2-3 most recently obtained 2D-kVs in which two or more fiducial positions have been successfully segmented. The information from the different 2D-kVs is weighted causing the model

to rely more heavily on the most recently obtained 2D-kV. The model is created and continously updated by optimizing the modelling parameters to minimize the difference between the most recently detected tumor position and the predicted tumor position by the model. The details behind the model formation are not published [12].

2.3.2 Uncertainty metric: Potential Difference

The system has a built-in uncertainty metric referred to as Potential Difference, which according to the manufacturer "can be interpreted as an estimate that is proportional to the standard deviation in the least certain direction for the next modeled target position". A threshold for this parameter can be set during treatment, and the fraction is interrupted if the threshold is exceeded [12].

2.3.3 Expected accuracy and latency

The manufacturer expects the root-mean-square error of Synchrony to be equal to or less than 1.5 mm when comparing the estimated trajectory of Synchrony to a known trajectory in a phantom. The latency between the system having determined a new tumor position and the MLC having reached the new positions commanded for shaping the adapted treatment beam is 45-55 ms [12].

2.4 Independent model for retrospective trajectory estimation

Poulsen et al. [10] have described a method for retrospective estimation of the trajectory of a prostate tumor using Kilovoltage Intrafraction Monitoring (KIM). KIM segments the projected tumor positions from the 2D-kVs obtained during treatment and uses all the found 2D positions and maximum likelihood estimation to estimate the 3D position.

2.5 Objective

Real-time target tracking and motion management have the potential to increase the accuracy of external beam radiotherapy which could allow for reduced target margins and thus better sparing of healthy tissue. To confidently rely on a real-time tumor tracking system, the tracking uncertainty and limitations must be known. This project aims to investigate the geometrical accuracy of Radixact Synchrony, an image-guided MLC-tracking system, in its detection of intrafractional translational prostate motion by comparison with Kilovoltage Intrafractional Monitoring (KIM), an independent retrospective model for trajectory estimation.

3 Methods

The method is based on modeling tumor trajectories retrospectively from programmed motion in a phantom as well as from 49 treatment sessions of seven patients with prostate tumors with three implanted gold fiducials. The fiducials were cylindrical with a radius 0.5 mm and a length of 5 mm.

3.1 Kilovoltage Intrafraction Monitoring (KIM)

The independent model used for retrospectively determining the tumor trajectory was Kilovoltage Intrafraction Monitoring (KIM), which has been described prevously by Poulsen et al [10]. A version of the model adapted to Synchrony's geometry implemented in Matlab by Per Poulsen was used for all testing.

3.1.1 Segmentation

KIM uses segmented fiducial positions from 2D-kV images to estimate the 3D position of the moving tumor. Segmentation is performed using normalized cross calibration with a digitally created template of the expected appearance of the fiducials. In patients, the fiducials are often angled due to difficulty positioning them in the compressible tissue of the prostate. Therefore, the angles at which the fiducials are placed were extracted by using Matlab's built in Blob function to find possible candidates in the 2D-kVs that could be fiducial projections and fitting a template tilted at different angles to the candidate projection. Fitting was performed for every treatment fraction for every patient and the angles found were used to generate the templates for segmenting the fiducial projections.

The position of the tumor projection is set to the mean of the positions of fiducials which have been successfully segmented. The criterion for a fiducial to be considered successfully segmented was that the correlation coefficient betweeen fiducial projection and template was larger than 0.32 as the segmentation method then managed to successfully separate fiducials from disturbances in the images.

3.1.2 Imager sag

During implementation of KIM on Synchrony, we found an oscillation in the KIM-estimated trajectory after adapting the model to the geometry on the Radixact. The oscillation was image angle dependent and mainly produced errors in the CC- and AP-directions, inducing a suspicion of an imager sag. A sag, or tilt, of some component

in the imaging system unknown to us, and therefore not accounted for when using the imaging system's geometry to recalculate the 2D projections into the 3D position, would produce this kind of angle dependant offset in the trajectory estimations. Since similar oscillations do not occur in Synchrony's estimations, the Synchrony system must know of and compensate for this sag. To handle this, the difference between the segmented marker positions by KIM and Synchrony was calculated for each image under the assumption that Synchrony's segmented marker positions were the same as the positions found when projecting down the 3D postion on the imager. The avarage of all differences for each imaging angle was then calculated and used to compensate for the sag in all of the images. This was done for every patient fraction.

3.1.3 Estimation of 3D tumor position

The unknown motion component is estimated by finding the distribution of tumor positions most likely to produce the found tumor projections. Assuming that the distribution of the tumor positions is Gaussian, the distribution can be described by the mean position in each direction of motion, the standard deviation in each direction of motion and the correlation coefficients of each motion direction pair. After segmentation, the found 2D positions are used to form a likelihood function constructed by multiplicating the probabilites associated with each individual projection, thus considering the joint probability of observing all the segmented positions. Maximising this joint probability yields the parameters describing the gaussian distribution.

At every imaging time point, the tumor is known to be located somewhere on the line between the kV-source and the projection point on the imager. Parametrizing this line and inserting it into the 3D probability density function (PDF) gives the 1D-PDF of the tumor position along the line. The expectation value of this 1D-PDF is used as the motion parameter parallell to the imager axis, see figure 7.

Since prostate motion exhibits a positive correlation between anterior and cranial directions, the 3D-PDF takes the shape of an ellipsoid with a tilted axis in the coordinate system. As a result, the standard deviation of the 1D-PDF used to estimate the unknown motion component varies at different estimation points depending on the angle of the imager at a given imaging point.

3.2 Phantom tests

In order to determine KIM's ability to accurately estimate tumor trajectories, the model was used to estimate known trajectories to which the estimated trajectories were then compared. This was done using 2D-kVs from sessions in which a phantom with three im-

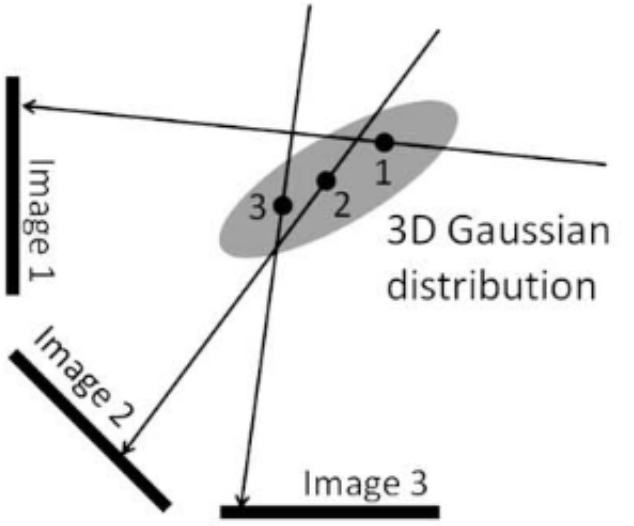

Figure 7: The tumor position is estimated as the mean position according to the 3D probability density function, illustrated as the gray ellipse, along the line between the kV-source and the projection point on the imager. Image source: Poulsen et al. with permission. [10]

planted fiducials put on a programmable motion stage (Delta4/Hexamotion) reproducing five previously published prostate trajectories [13] had been placed in the Radixact. The offsets caused by the imager sag were calculated for each phantom trace and the mean offset at each imaging angle was subtracted from the segmented tumor positions. KIM estimated the trajectory using the segmented positions from the 2D-kVs obtained during the sessions and the trajectories were compared to the programmed motion of the phantom motion stage as well as the trajectory Synchrony had recorded during the session. The estimation errors were related to the motion velocity, which was estimated as the slope between the time point of the investigated difference and the previous time point.

Due to the difficulties in timing the motion start of the phantom motion stage and imaging start in Radixact, the Synchrony and KIM estimated trajectories whose time stamps are based on the imaging system in Radixact were shifted in relation to the phantom motion. This timeshift was handled by visually determining the time delay between the systems. This affects the comparisons made between Synchrony and phantom as well as KIM and phantom. It does however not affect the comparisons made between KIM and Synchrony since the two models are based on the same time stamps.

3.3 KIM and Synchrony on patient data

2D kVs and tumor trajectories as estimated by Synchrony during treatment of seven patients were obtained. The offsets caused by the imager sag were calculated for each

imaging angle and fraction, and the avarage offset at each imaging angle was subtracted from the tumor positions segmented by KIM. The motion in each fraction was analyzed and summarized in boxplots for each patient, fraction and motion component.

The differences between the KIM- and Synchrony estimations were analyzed to find potential sources of estimation differences. The distribution of the differences in each motion direction was summarized in histograms and in scatter plots with the size of the differences in each motion direction was related to the size of the 3D differences. This was done twice; with and without compensation for the offset attributed to the error introduced by the uncertainty in fiducial marker identification during production of the synthetic CT. Compensation was done by finding the avarage differences of the the segmented marker positions by KIM and Synchrony and subtracting it from the marker positions KIM found. This was done for each individual marker.

3.4 Statistics

Mean root-mean-square difference (RMSD) was calculated between KIM-estimated trace and phantom motion, and synchrony-estimated trace and phantom motion for all phantom tests. Mean RMSD was also calculated between Synchrony-estimated trace and KIM-estimated trace for both phantom and patient tests. Mean standard deviation (SD) of the differences and the 99th percentile difference was also computed for each comparison. The SD in the patient tests was calculated by taking the sqareroot of the added, quadrated means of the SDs over all fractions for each patient. All calculations were performed in Matlab R2023a (MathWorks Inc., USA).

3.5 Verifictation of Synchrony's uncertainty parameter

Synchrony's abilty to catch its own estimation errors was also analyzed by plotting the variation of the uncertainty parameter potential difference together with the calculated differences between Synchrony's trajectory estimation and the programmed trajectory of the phantom for phantom tests, and the estimation differences between KIM and Synchrony in patients.

4 Results

4.1 KIM and Synchrony vs phantom

All pre-programmed traces of previously recorded prostate motion contained high dynamic in the CC- and AP-directions. Both KIM and Synchrony estimated the trajectories within sub-millimeter RMSD in all motion directions when compared to the programmed motion of the phantom. The 3D RMSD between KIM and phantom was 0.77 mm with a mean SD of 0.30 mm, and the 3D RMSD between Synchrony and phantom was 0.82 mm with a mean SD of 0.47 mm. The larger RMSD in the 3D difference between Synchrony and phantom trace when compared to that between KIM and phantom trace is due to a larger difference in the LR-direction for Synchrony's estimations, see table 1.

In general, the errors of Synchrony's calculated position were more condensed, especially in the AP direction, compared to those of KIM judging by the smaller interquartile ranges shown in the boxplot in figure 8. However, Synchrony made larger estimation errors than KIM as shown by the larger SD in the errors of Synchrony and the 99th percentile of the errors: 99 % of the 3D differences between estimation and the phantom motion was smaller than 1.70 mm for KIM and smaller than 3.54 mm for Synchrony, see table 1.

In all of the phantom traces, the Synchrony-estimated trace tended to oscillate in the LR-direction in conjunction with rapid movement in the CC- and/ or AP-direction, see figure 9a between t = 100 s and t = 130 s, and at t = 220 s and figure 9b at t = 130 s and t = 210 s. The size of the oscillations are between 1 and 2 mm. Synchrony also tended to react slower to AP motion than KIM, causing a delay in the Synchrony-estimated trace when compared to the KIM-estimated trace which can be observed in the AP directions at the same time stamps as the LR-oscillations in figure 9a and b. The relationship between large errors and rapid motion is illustrated in figure 10.

Table 1: The mean root-mean-square difference (RMSD), mean standard deviation (SD), and the 99th percentile of the differences between the programmed motion of the phantom and the Synchrony-estimated trajectories and the KIM-estimated trajectories respectively in left-right (LR), cranio-caudal (CC), anterio-posterior (AP) directions as well as the total three dimensional motion (3D).

		LR (mm)	CC (mm)	AP (mm)	3D (mm)
Mean RMSD	KIM vs phantom	0.31	0.28	0.64	0.77
	Synchrony vs phantom	0.42	0.26	0.65	0.82
Mean SD	KIM vs phantom	0.26	0.23	0.41	0.30
	Synchrony vs phantom	0.36	0.21	0.49	0.47
99th percentile	KIM vs phantom	0.83	0.48	1.32	1.70
	Synchrony vs phantom	1.67	0.39	2.68	3.54

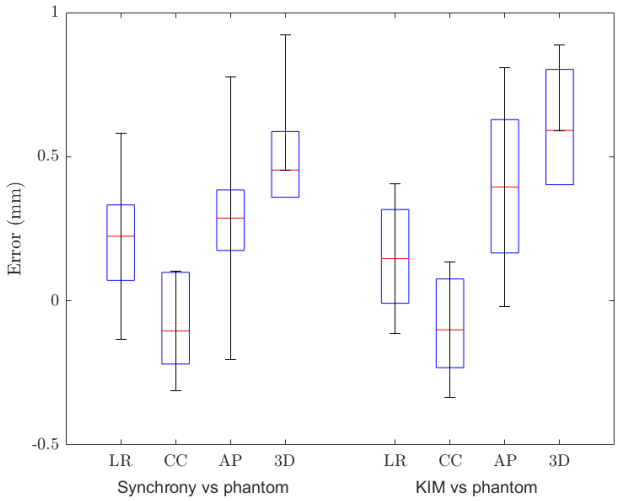

Figure 8: The errors of Synchrony's and KIM's estimations of the phantom traces in left-right (LR), cranio-caudal (CC), anterio-posterior (AP) directions as well as the total three dimensional motion (3D). The boxes contain the interquartile range, the red lines mark the median errors and the whiskers represent the mean standard deviations.

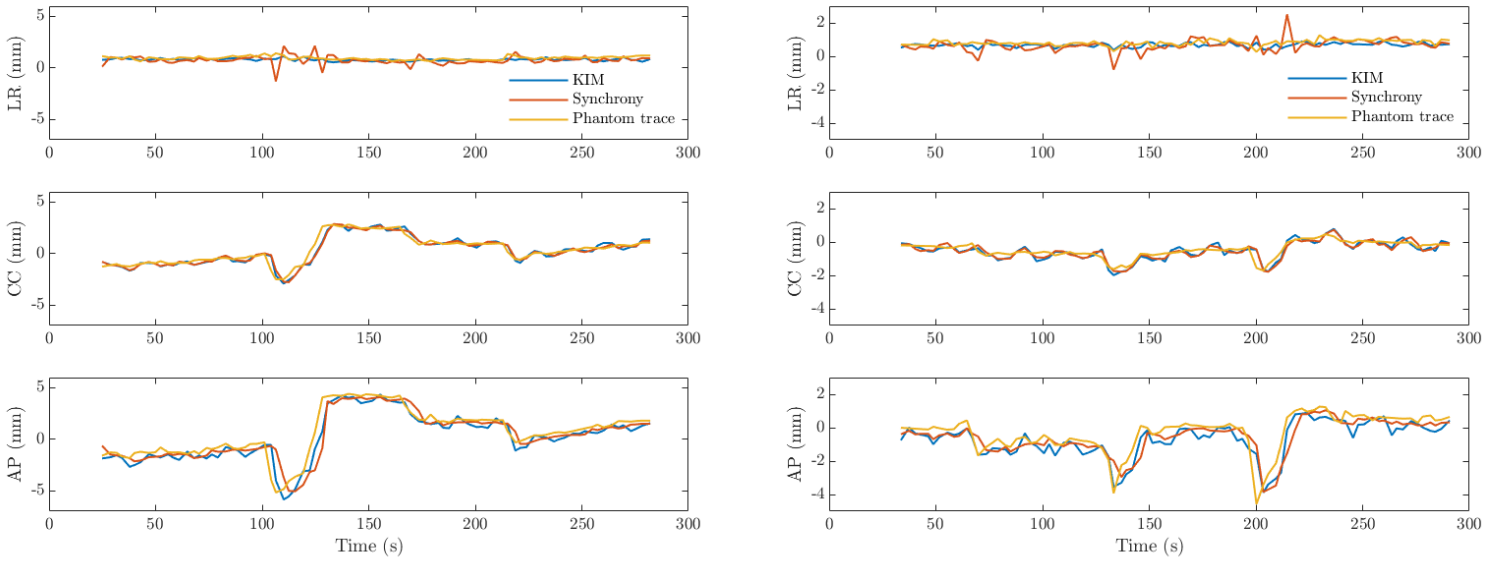

(a) (b)

Figure 9: Visualization of the phantom trace motion (yellow), the motion estimated by Synchrony (red) and KIM (blue) in left-right (LR), cranio-caudal (CC) and anterior-posterior (AP) directions.

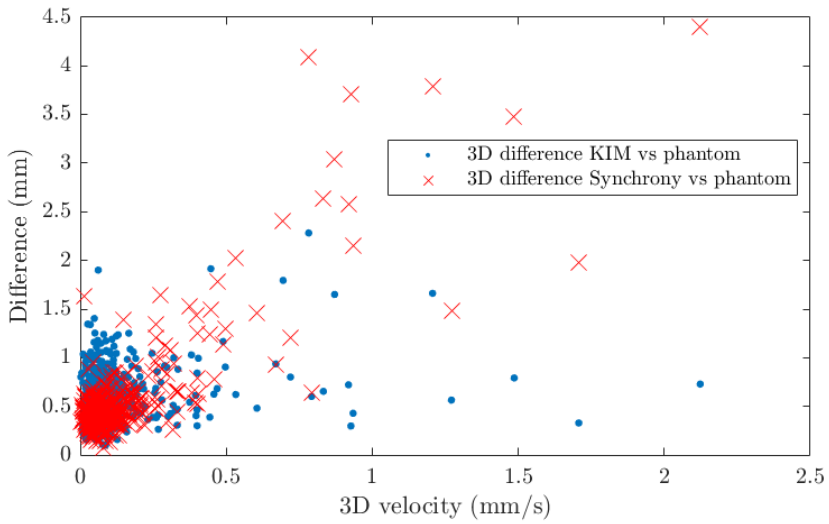

Figure 10: The calculated 3D difference between phantom and KIM-estimated traces (blue dots) and the 3D difference between phantom and Synchrony-estimated traces (red crosses) in time point N+1 related to the momental 3D velocity as calculated by the slope between time points N and N+1 in the phantom motion.

4.2 KIM and Synchrony in patients

2D-kVs and the tumor trajectories as estimated by Synchrony during treatment of seven patients with an age over 40 treated for prostate adenocarcinoma at Skånes Universitetssjuhus during 2023 were acquired from the system. All patients had three fiducial markers implanted in the prostate and the treatment of each patient consisted of radiation dose of 42.7 Gy delivered during seven fractions with a delivery of 6.1 Gy per fraction, three fractions per week. The treatment was delivered on a Radixact machine with the motion tracking system Synchrony, both manifactured by Accuray.

Out of 49 fractions, 8 were excluded in the data analysis due to missing data or file reading errors. In the remaining 41 fractions the prostate remained fairly static in the majority of the fractions, as seen in figure 15, 16 and 17 in appendix A, showing the deviations from the initial tumor position in each motion direction as estimated by KIM and Synchrony respectively. In eight fractions, large movements appeared. In three of those fractions, the motion was a slow drift in the inferior and posterior directions occuring throughout the entire fraction, likely caused by bladder filling. In the rest of the fractions, the motion was rapid and in the superior and anterior direction, most likely caused by movements of the rectum.

The estimated trajectories of KIM and Synchrony was in agreement for all patient traces and the 3D RMSD between the KIM- and Sychrony-estimated traces over all patient fractions were 1.03 mm with a SD of 1.17 mm. The 3D differences between the estimated trajectories by KIM and Synchrony were smaller than 2.61 mm 99 % of the time, see table 2. In addition, the differences and mean SD are visualised in the boxplot in figure 11. In four of the patients, an offset of about 0.5-1 mm could be observed between the KIM- and Synchrony-estimated trajectories in the CC-direction.

Table 2: The mean root-mean-square difference (RMSD), mean standard deviation (SD) of the difference, and the 99th percentile of the differences between the Synchrony-estimated trajectories and the KIM-estimated trajectories in left-right (LR), cranio-caudal (CC), anterio-posterior directions as well as the total three dimensional motion (3D). All values are in millimeters.

Difference KIM vs Synchrony	LR (mm)	CC (mm)	AP (mm)	3D (mm)
RMSD	0.37	0.77	0.52	1.03
Mean SD	0.92	1.22	1.30	1.17
99th percentile	1.23	1.22	2.02	2.61

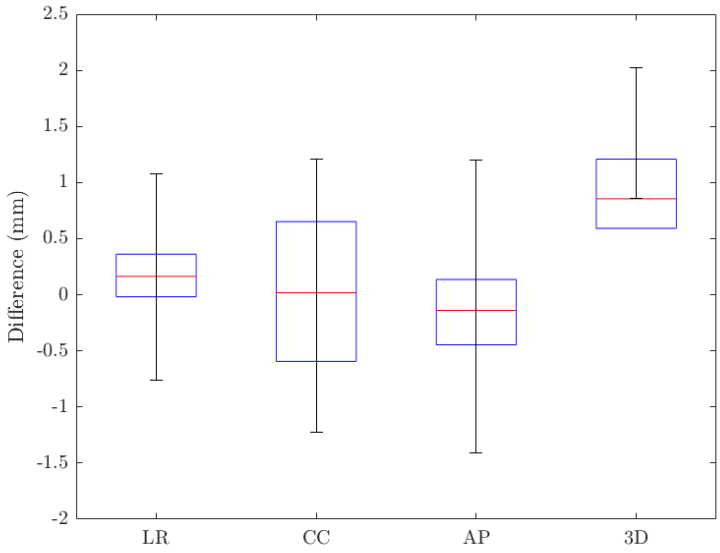

Figure 11: The differences between Synchrony's and KIM's esitmations of the patient traces in each direction of motion. The boxes contain the interquartile range, the red lines mark the median errors and the whiskers represent the mean standard deviations.

In the fractions where motions were observed, Synchrony tended to oscillate in conjunction with rapid movement in the CC- and/or AP-direction, see figure 12a between t = 50 s and t = 100 s, and in figure 12b at t = 90 s. The Synchrony-estimated trajectory also exhibited a delay of around 4 s in AP during rapid motion when compared to the KIM-estimated trace, which can be observed at t = 50 in figure 12a and t = 90 s in 12b.

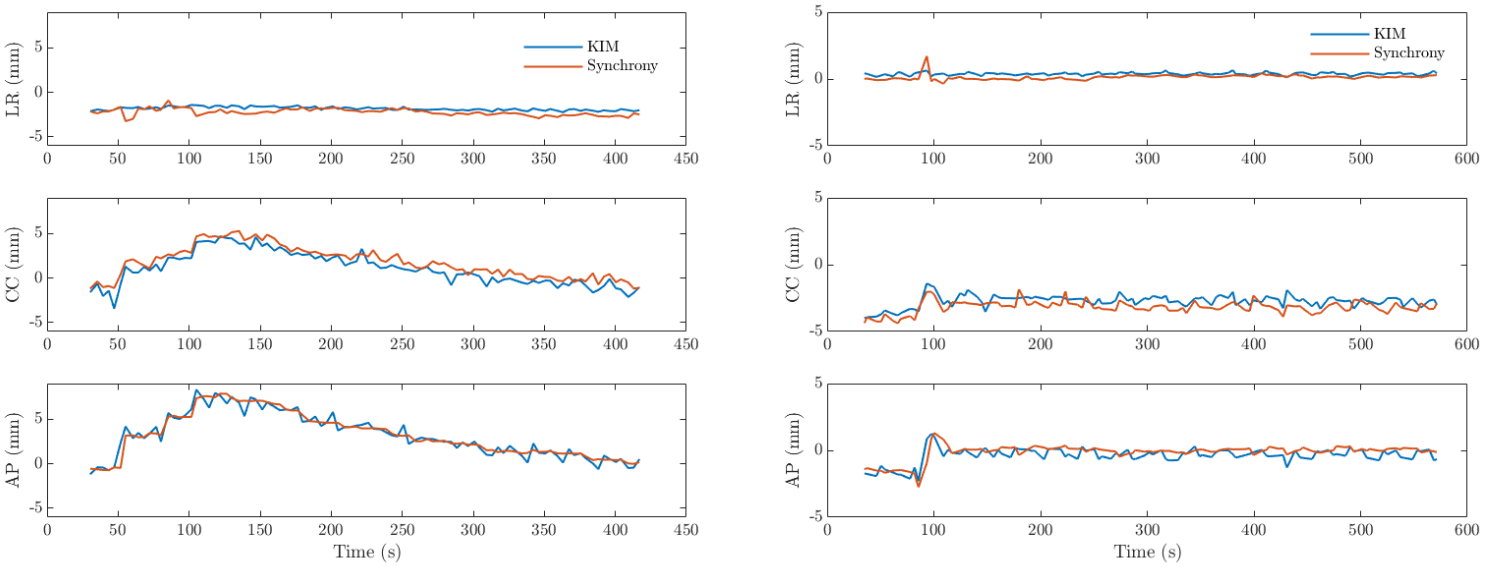

(a) (b)

Figure 12: Visualization of the motion of a prostate tumor in a patient as estimated by Synchrony (red) and KIM (blue) in left-right (LR), cranio-caudal (CC) and anterior-posterior (AP) directions.

4.3 Analysis of differences in estimated motion

The differences between the KIM- and Synchrony-estimated trajectories mainly appeared in the CC- and AP-direction where it was up to 2.5 mm and 2 mm respectively. After compensating for the offset observed in CC, the difference between KIM and Synchrony was up to around 1 mm in CC and remained up to 2 mm in AP. The spread of the differences in LR decreased after compensation, however the large deviations remained the same size, see figure 13.

The differences in each respective motion-direction were also plotted against the 3D difference both with and without offset compensation. Without offset compensation, the 3D difference is formed by errors in all motion directions, see figure 14a. With offset compensation, the main part of the 3D difference is caused by differences in LR and AP. Many of the large differences are formed almost entirely by estimation differences in AP, see figure 14b.

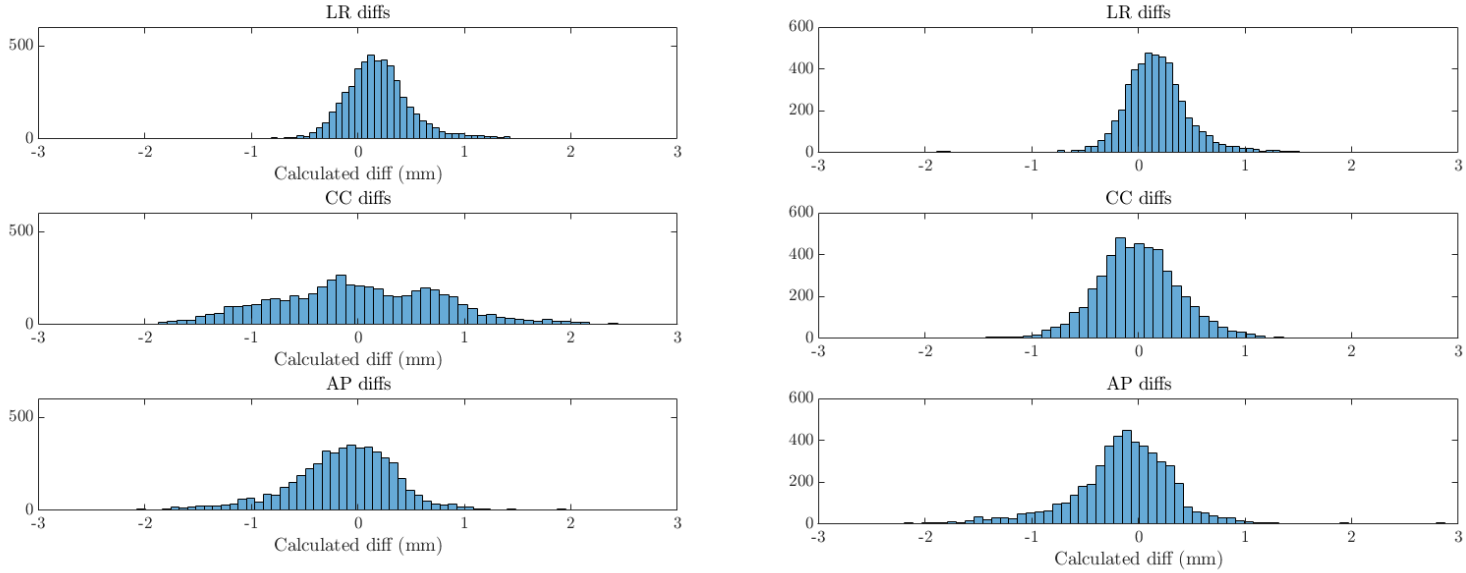

(a) Uncompensated (b) Compensated

Figure 13: Histogram of the differences between the KIM- and Synchrony-estimated trajectories of prostate tumor motion in patients in left-right (LR), cranio-caudal (CC) and anterior-posterior (AP) directions. a is uncompensated and b is compensated for the offset between the estimations.

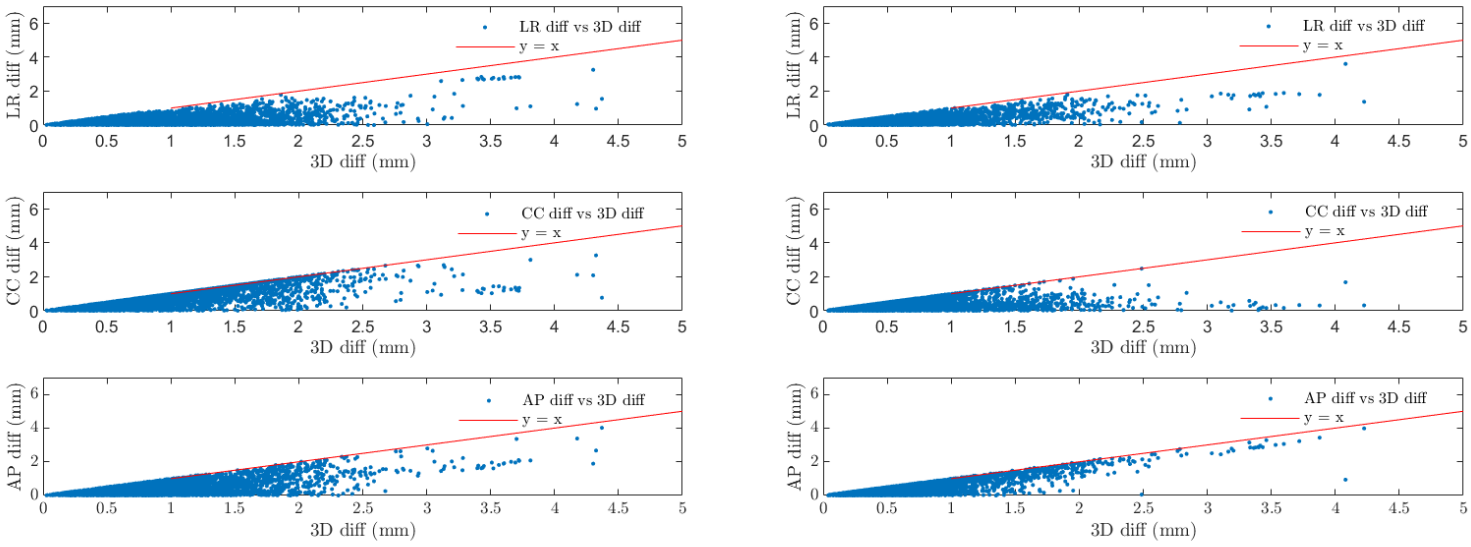

(a) Uncompensated (b) Compensated

Figure 14: The difference between the KIM- and Synchrony-estimated trajectories in LR, CC and AP plotted against the 3D difference together with the line y = x in red. a is uncompensated and b is compensated for the offset between the estimations.

4.4 Verification of Synchrony's uncertainty parameter

Plotting Synchrony's built in uncertainty parameter Potential Difference together with the differences between the trajectory estimations made by KIM and Synchrony in patients or the error between Synchrony's estimations in phantoms shows an increase in the potential difference when the rapid movement occurs. See figure 18 and figure 19 in appendix B. An increase in the estimation difference/ error is accompanied by an increase in potential difference.

5 Discussion

5.1 KIM's usefulness as a model for verifying Synchrony

The implementation of KIM on Synchrony was successful and the RMSD between KIM-estimated trajectory and pre-programmed phantom trace was sub-millimeter in all motion directions. Synchrony's estimations also resulted in a sub-millimeter RMSD between estimation and phantom trace in agreement with the accuracy expected by the manufacturer, however the RMSD was notably larger than for KIM in LR-direction. KIM is deemed useful as an independent model for verifying Synchrony's accuracy in estimating tumor trajectories in patients.

5.2 Estimation differences between KIM and Synchrony

Large differences in Synchrony's estimations of the trajectories produced by phantom occured in conjunction with rapid motion as shown in figure 10. The same behaviour could be observed when visually inspecting the Synchrony-estimated trajectories in the treatment sessions of patients, however a correlation could not be shown quantitatively between the differences in estimations between KIM and Synchrony and the velocity of the trajectory. This is probably due to the challenge of calculating the velocity of the tumor, since the actual trajectory of the tumor is not known. Estimating the velocity as the slope of the KIM- or Synchrony estimated traces between two imaging time points is inaccurate as the velocity will then be affected by the noise in both trajectory estimations. Averaging over several imaging time points and thereby position estimations instead introduces the risk of missing rapid motion since the entire motion sometimes occurs between few imaging time points and the tumor quickly moves back to a position close to where it started.

5.2.1 Differences in cranio-caudal motion estimation

KIM's and Synchronys estimation of the CC-motion was in good agreement in regards to the shape of the estimated trajectories. Both models are expected to have good estimations of the movement in CC, since the movement occuring in this direction is perpendicular to the imager axis and therefore entirely visible to the system. However, there was an offset between the trajectories resulting in an RMSD between the two models' estimations that was largest in CC. This offset is compensated for during the analysis of the errors as explained in the method. After compensation, the vast majority of the estimation differences in CC are below 1 mm and most likely caused by noise in

the estimated trajectories, see figure 13b.

When compensating, there is a risk that compensation also is made for other, unknown, systematic errors in the system's segmentation method. The observed offsets behaved in the way expected of the offset that would appear due to errors in the fiducial marker position identification when generating the synthetic CT used for treatment planning: the offset was not the same for all patients, but remained the same size between the treatment fractions for each patient. This is expected since the offset is introduced in the treatment plan, which is then used for all fractions. In addition, Synchrony did not exhibit any offset in the estimation of the phantom motion in which no synthetic CT was used to establish the initial positions of the markers. It is therefore very likely that the compensation only accounts for the error introduced by the uncertainty in the generation of the synthetic CT, since other systematical errors would appear in the phantom trajectory estimations as well.

5.2.2 Differences in anterior-posterior motion estimation

The large 3D differences between the KIM- and Synchrony-estimated trajectories seem to mainly be caused by differences in AP after compensating for the offset, see figure 14b. These large differences appear due to the delay in the estimation of tumor motion in Synchrony when compared to KIM. KIM is expected to respond quicker to motion in general, since the model works retrospectively and has knowledge of the entire trajectory in each point of estimation. Since Synchrony works by determining the motion using the three most recent 2D-kVs, it is expected to estimate the movement with a bit of a delay. The delay could however also be due to an overestimation of the correlation of motion in CC and AP in KIM, which then falsly estimates a movement in CC followed by a movement in AP as movement in both motion directions occuring simultanously. The majority of the delay is however more likely to be caused by Synchrony's model having a delay in the motion estimation.

5.2.3 Differences in left-right motion estimation

The trajectory estimations in LR were very similar between KIM and Synchrony and exhibited very limited motion apart from some oscillation in the Synchrony-estimated trajectory in conjunction with rapid movement in the other motion directions. Since the prostate is not expected to move in the LR direction and the same behaviour was observed in Synchrony's estimation of phantom motion where it is known that no LR motion occurred, the conclusion can confidently be made that the larger differences between KIM and Synchrony estimations are due to errors in the Synchrony estimation.

5.3 Potential improvements to the Synchrony model

Synchrony's slower response to AP motion and the oscillations in LR imply that Synchrony's model does not take known aspects of prostate motion into account, namely the correlation between CC and AP motion. The model seems to expect detected CC motion to be accompanied by motion in other motion directions, but it does not know which one. This could be the explainaition behind the oscillations in LR and the delayed response in AP. The model needs additional 2D-kVs before it can determine which other motion direction is involved in the motion. Adjusting the model to expect a correlation between CC and AP motion could potentially improve its estimations and rid the model of the LR oscillations and AP delay.

5.4 Does Synchrony catch its errors?

The built in uncertainty parameter Potential Difference increases as estimation errors increases, showing that Synchrony has good insight in when its estimations are uncertain. This has been visually determined by examining all trajectories in plots such as those in Appendix B. Efforts were made to quantitatively verify that the errors are caught by Synchrony and lie within the estimated potential difference, but no method was sufficient with the data available for this project. Comparisons made between phantom motion and Synchrony's estimation are affected by the time shift between the phantom and Synchrony and can not be used unless the delay between the two time systems is known, and comparisons in patient cases are unreliable as it is impossible to determine whether the differences in trajectory estimations are caused by errors in KIM's or Synchrony's estimations. Further investigations should be made to numerically determine the accuracy of the potential difference.

5.5 Implications for delivered dose

The LR oscillations are small and only present for very short time periods and are therefore unlikely to affect the delivered dose. The delay in AP combined with the latency in the Synchrony system could result in the treatment beam being misdirected throughout the entire motion, since the tumor will have had time to move from the new estimated position once that estimation has been made. However, since rapid motion of the prostate only appears for a few seconds per fraction in only a few fractions, realistically the treatment beam should not be misdirected for more than a few seconds due to the delay. Rapid motion occuring over a longer time period would most likely also be reflected in a growing potential difference the longer the motion has occured, resulting in the potential difference eventually exceeding the set threshold and the system

interrupting the treatment.

The size of the estimation errors when comparing Synchrony to the pre-recorded phantom trace as well as the differences between KIM's- and Synchrony's estimations were notably smaller than the treatment margins of 7 mm used today. The estimation errors Synchrony makes would therefore not impact the delivered dose if the same target margins were used. Judging by the 99th percentile of estimation errors in Synchrony, almost halving the margin would mean that the tumor position is within the PTV 99 % of the time if only translational motion is expected.

6 Conclusion and further investigations

Synchrony's model accurately estimates the intrafractional translational motion of the prostate during treatment of patients and could be used to reduce target margins. The errors that do appear develop in conjunction with rapid movement and are transient and smaller than the treatment margins used today. The estimation made by Synchrony could be improved and the treatment margins thus reduced further by including a correlation between CC and AP motion in the model.

Further investigations looking at a larger patient population should look into how rapid the motion resulting in estimation errors is and how frequently this kind of motion occurs in order to determine more precisely how much the motion impacts delivered dose and thus how large the target margins must be. Synchrony's handling of other types of prostate motion and changes that can occur during treatment, such as rotation and swelling, should also be studied to see if the system can account for these changes as well.

7 References

References

[1] Lehtonen M, Kellokompu-Lehtinen PL. The past and present of prostate cancer and its treatment and diagnostics: A historical review. SAGE Open Med. 2023;11.

[2] National Cancer Institute. Radiation Therapy to treat cancer [Internet]; 2019-01-08; 2019. Accessed 2023-12-16. Available from: https://www.cancer.gov/about-cancer/treatment/types/radiation-therapyHRTWAC.

[3] Pommer T. Real-time motion management of prostate cancer radiotherapy [dissertation]. Faculty of Science, University of Copenhagen; 2014.

[4] Regionala cancercentrum i samverkan. Yttre strålbehandling av prostata med guldkorn eller guldankare [Internet];2021-05-12; 2021. Accessed: 2023-12-22. Available from: https://cancercentrum.se/globalassets/cancerdiagnoser/prostatacancer/min-vardplan/diagnos-och-behandling/yttre-stralbehandling-av-prostata-med-guldkorn-eller-guldankare.pdf.

[5] Bortfeld T. IMRT: a review and preview. Physics in medicine and biology. 2006;51(13).

[6] Britannica Academic, Encyclopædia Britannica. Radiation Therapy [Internet];2018-12-07; 2018. Accessed: 2023-12-22. Available from: https://academic-eb-com.ludwig.lub.lu.se/levels/collegiate/article/radiation-therapy/62401.

[7] US government agency National Cancer Institute. Prostate and bladder, sagittal section [Internet]; 2006. Accessed: 2023-12-26. Available from: https://upload.wikimedia.org/wikipedia/commons/a/a1/Prostatelead.jpg.

[8] Persson E, Gustafsson CJ, Ambolt P, Engelholm S, Ceberg S, Bäck S, et al. MR-PROTECT: Clinical feasibility of a prostate MRI-only radiotherapy treatment workflow and investigation of acceptance criteria. Radiation Oncology. 2020;15(77).

[9] Dang A, Kupelian PA, Cao M, Agazaryan N, Kishan AU. Image-guided radiotherapy for prostate cancer. Translational Andrology and Urology. 2018;7(3).

[10] Poulsen PR, Cho B, Keall PJ. A method to estimate mean position, motion magnitude, motion correlation, and trajectory of a tumor from cone-beam CT projections for image-guided radiotherapy. International Journal of Radiation Oncology, Biology, Physics. 2008;75(5):1587-96.

[11] Wikimedia Commons. Multi leaf collimator[Internet]; 2006. Accessed 2023-12-26. Available from: https://commons.wikimedia.org/wiki/File:Multi_leaf_collimator.jpg.

[12] Accuray Incorporated. Synchrony on the Radixact Treatment Delivery System; 2021.

[13] Ballhausen H, Li M, Belka C. The ProMotion LMU dataset, prostate intra-fraction motion recorded by transperineal ultrasound. Scientific Data. 2019;6(1):269.

A Appendix A

Prostate motion in patient fractions

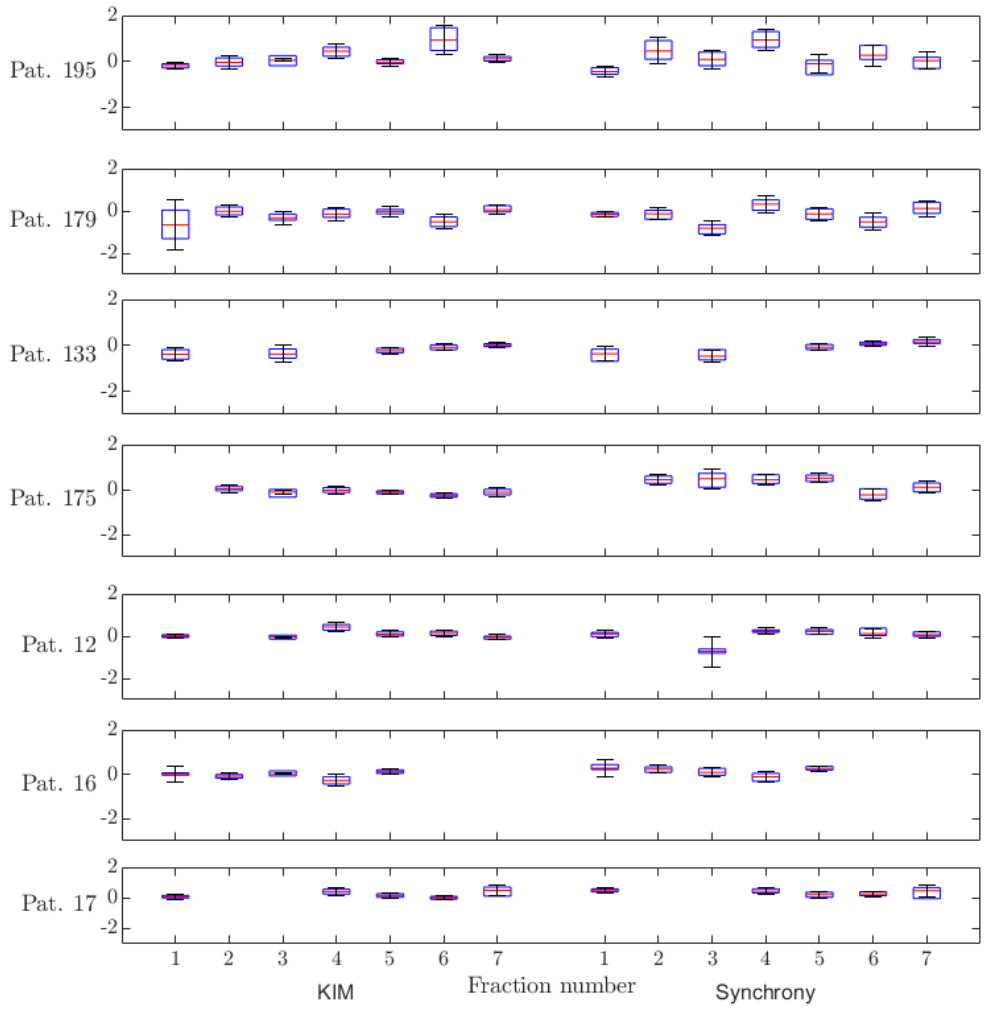

Figure 15: Box plot of the deviation from the initial tumor position in the left-right direction for each patient and treatment fraction. The box contains the inter quartile range, the red line represents the median deviation and the whiskers represent the standard deviation.

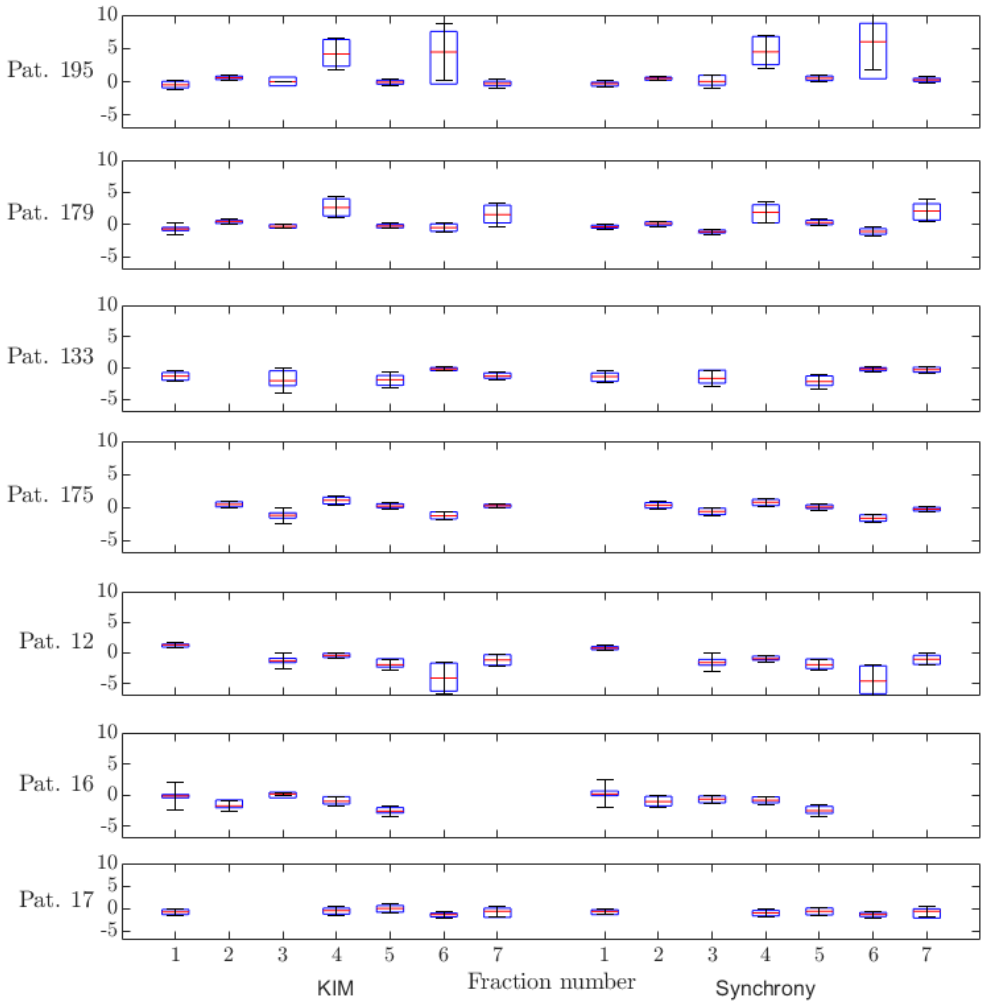

Figure 16: Box plot of the deviation from the initial tumor position in the cranio-caudal direction for each patient and treatment fraction. The box contains the inter quartile range, the red line represents the median deviation and the whiskers represent the standard deviation.

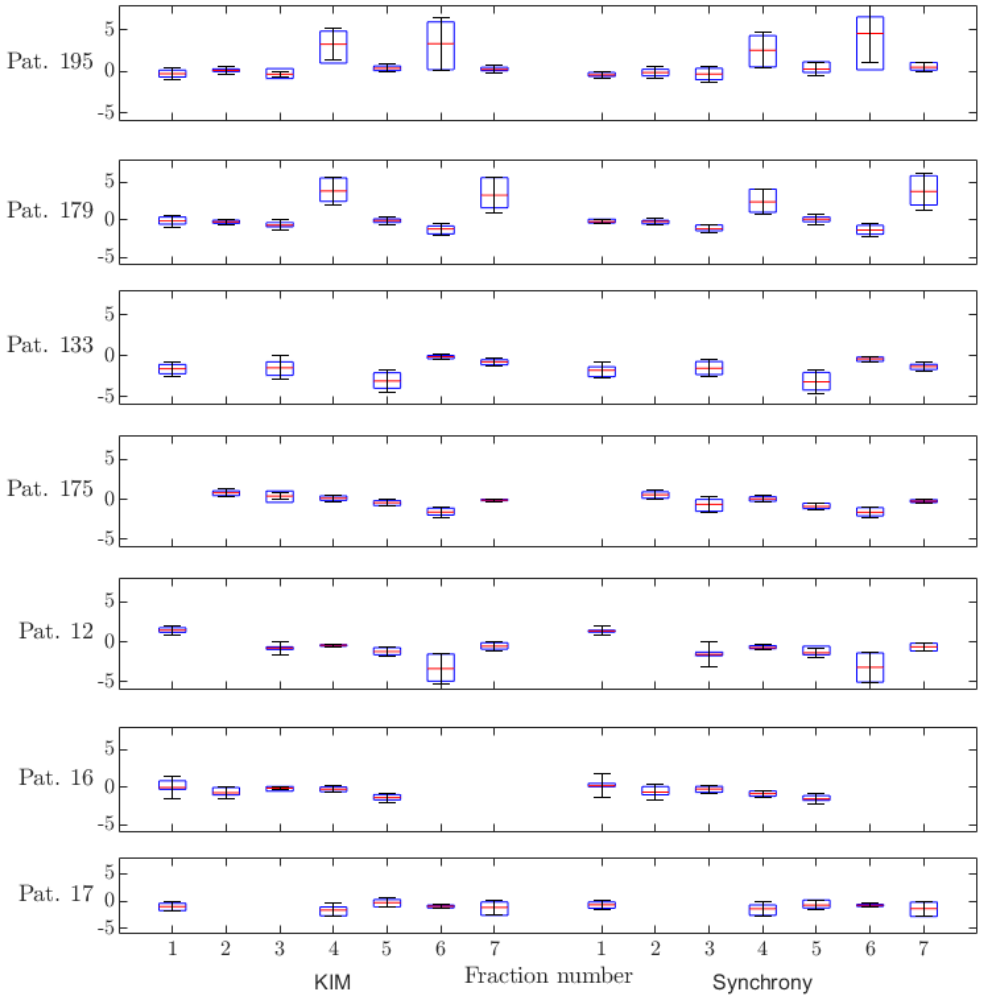

Figure 17: Box plot of the deviation from the initial tumor position in the anterior-posterior direction for each patient and treatment fraction. The box contains the inter quartile range, the red line represents the median deviation and the whiskers represent the standard deviation.

B Appendix B
Potential Difference in fractions with rapid motion

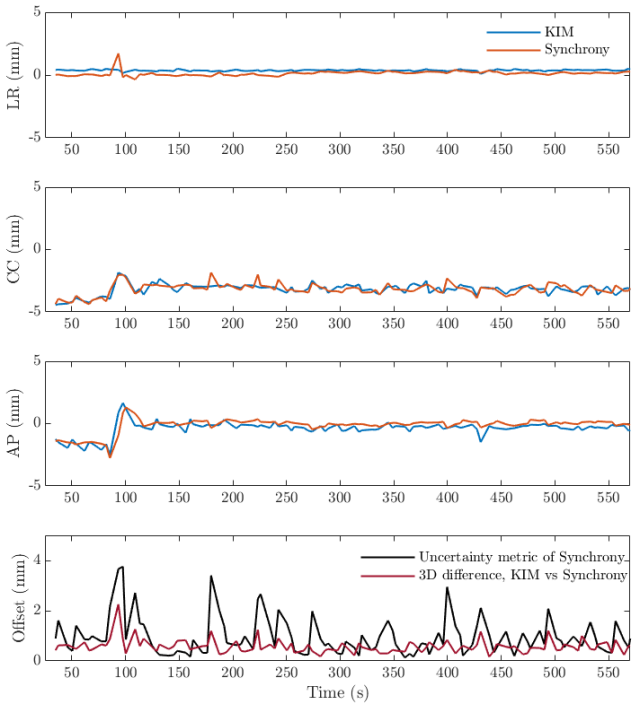

(a) Patient 12, fraction 1

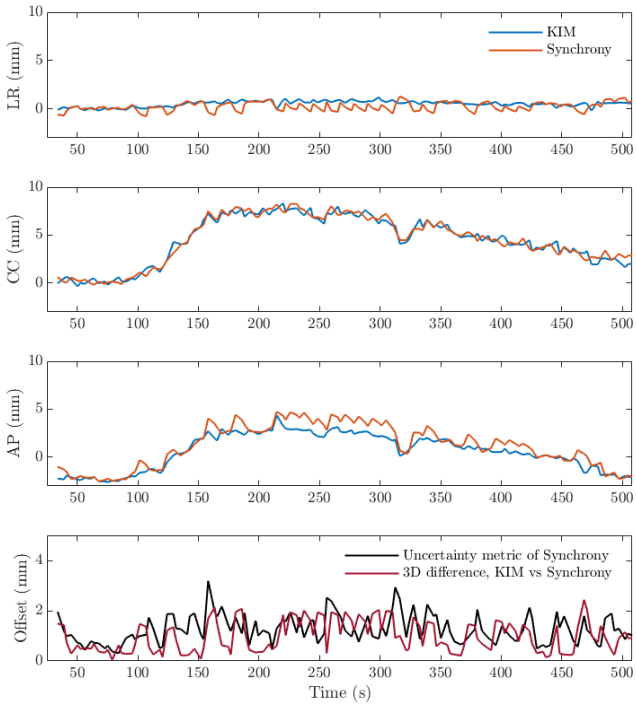

(b) Patient 195, fraction 4

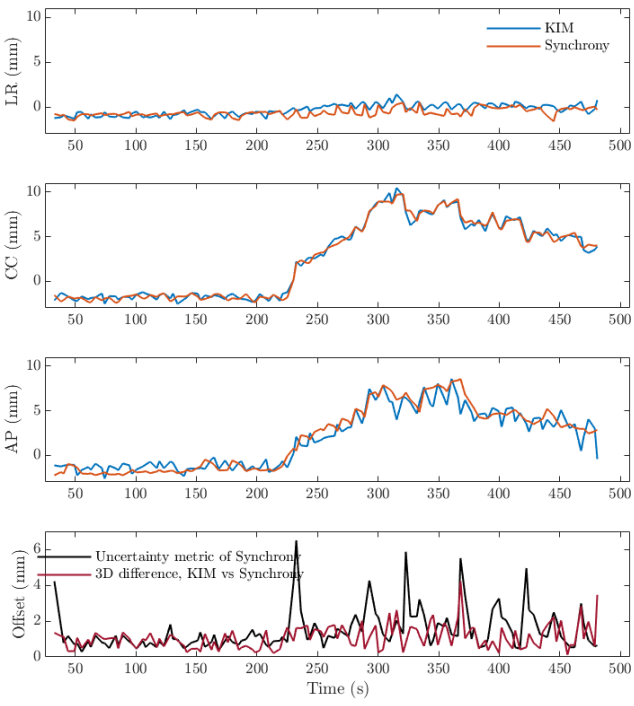

(c) Patient 195, fraction 2

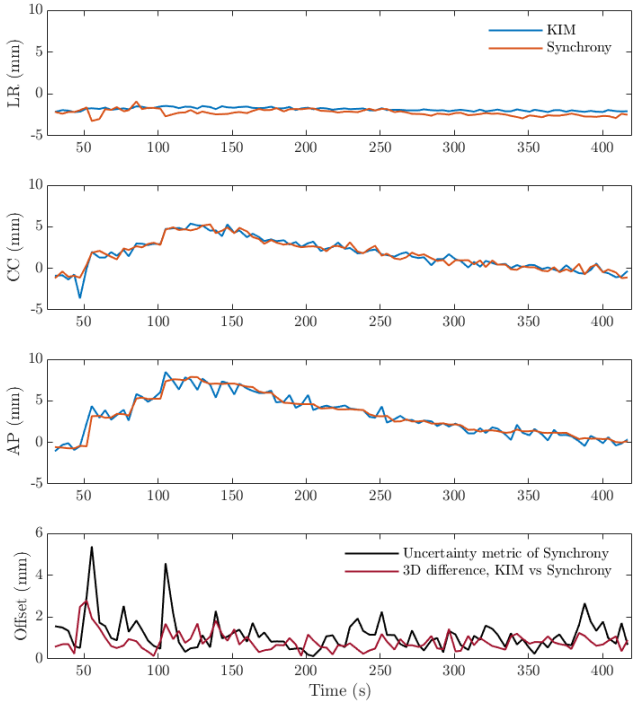

(d) Patient 179, fraction 7

Figure 18: Visualization of the motion (top three subfigures in each figure) with the motion estimated by Synchrony (red) and KIM (blue) in left-right (LR), cranio-caudal (CC) and anterior-posterior (AP) directions. Bottom shows the uncertainty metric of Synchrony (black) versus the calculated 3D difference between Synchrony- and KIM-estimated trace (red).

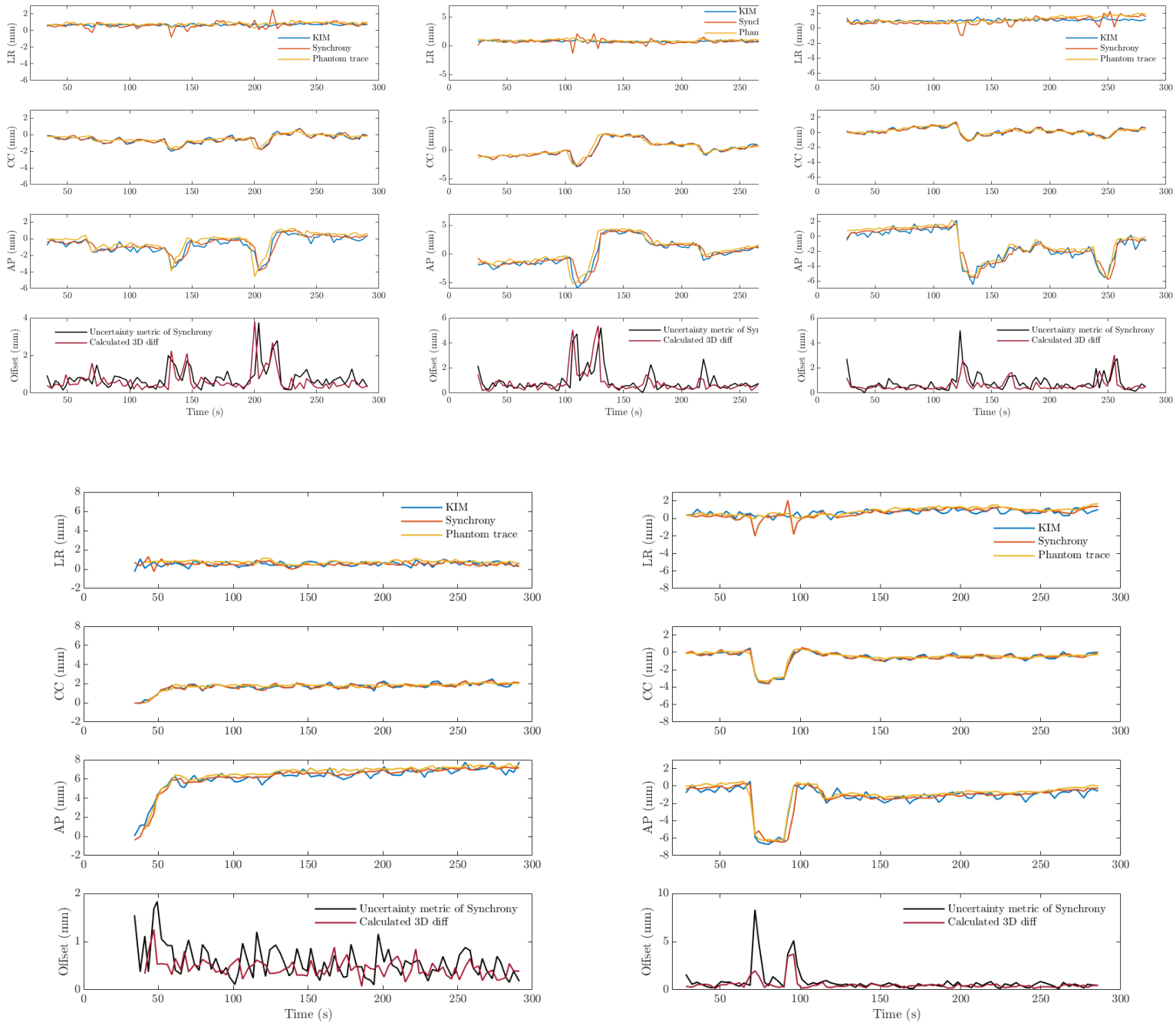

Figure 19: Visualization of the motion (top three subfigures in each figure) with phantom trace (yellow), the motion estimated by Synchrony (red) and KIM (blue) in left-right (LR), cranio-caudal (CC) and anterior-posterior (AP) directions. Bottom shows the uncertainty metric of Synchrony (black) versus the calculated 3D difference between Synchrony- and KIM-estimated trace (red).